Journal of King Saud University - Science 35 (2023) 102999

HOSTED BY

Contents lists available at ScienceDirect

Journal of King Saud University - Science

journal homepage: www.sciencedirect.com

Micromeria biflora mediated gold and silver nanoparticles for colourimetric detection of antibiotics and dyes degradation

Naeem Khan [a,*], Fakhra Kalsoom [a], Nargis Jamila [b,*], Shaukat Shujah [a], Azhar Ul-Haq Ali Shah [a], Umar Nishan [a], Muhammad Ishtiaq Jan [a], In Min Hwang [c], Mohamed S. Elshikh [d], Riaz Ullah [e,*]

[a] Department of Chemistry, Kohat University of Science and Technology, Kohat 26000, Khyber Pakhtunkhwa, Pakistan
[b] Department of Chemistry, Shaheed Benazir Bhutto Women University, Peshawar 5000, Khyber Pakhtunkhwa, Pakistan
[c] Fermentation Regulation Research Group, World Institute of Kimchi, Gwangju, Republic of Korea
[d] Department of Botany and Microbiology, College of Science, King Saud University, Riyadh 11451, Saudi Arabia
[e] Department of Pharmacognosy, College of Pharmacy, King Saud University, Riyadh 11451, Saudi Arabia

ARTICLE INFO

Keywords:
Micromeria biflora
MBAuNPs
MBAgNPs
Methylene blue
Amoxicillin

ABSTRACT

The study reports on synthesis of aqueous extract mediated gold and silver nanoparticles of *M. biflora* (MBAuNPs and MBAgNPs) via hydrated chloroauric acid and silver nitrate salts. The nanoparticles (NPs) were produced in 1:15 (MBAuNPs) and 1:6 (MBAgNPs) ratios under sunlight displaying localized surface plasmon resonance (LSPR) peaks at 541 and 431 nm, respectively. The sizes characterized by transmission electron, scanning electron, and atomic force microscopic (SEM, TEM, AFM) techniques were respectively 26.73 nm and 53.81 nm. The subject NPs demonstrated application in the degradation of methylene blue, Congo red, Rhodamine B, methyl orange, *ortho*-nitrophenol, and *para*-nitrophenol ranging from 65 to 86 %. For detection of levofloxacin, amoxicillin, and azithromycin antibiotics, the MBAuNPs and MBAgNPs exhibited efficiency in real water and biological (blood plasma and urine) samples. Conclusively, the MBAuNPs and MBAgNPs applications for dyes degradation and antibiotics detection was found as simple and cost-effective analytical method.

1. Introduction

Designing simplest structures of nanoparticles (NPs) of size from 1 to 100 nm generate a mechanism with novel research and fundamental functionalities, strategies, and methodologies. These are the extreme economically altering material features, and generally of proficient degree for advanced in addition to molecular levels (Ansari et al., 2022). Green synthesis protocols, in particular, by using various common and low-cost sources such as plant and fruit extracts, as stabilizing agents for preparation of nanomaterials is the modern research trend of the scholars from around the world. The plant extract mediated synthesis of NPs have several key advantages over chemical nano-synthesis methods as being economically efficient and environmental friendly (Pirtarighat et al., 2019). Using aqueous extract of various plants in the synthesis of several metal nanoparticles have been reported as an acceptable alternative to physicochemical processes of NPs synthesis (Salem & Fouda, 2021).

Metals such as gold and silver are mostly used to synthesize stable dispersed nanoparticles, which are useful in photography, catalysis, optoelectronics, bio-marking, nanoscale biotechnology, and biomedical sciences (Báez et al., 2021). Gold nanoparticles (AuNPs) have been used in the detection of a polynucleotide or protein, immunoassay, cancer nanotechnology (especially cancer cell detection), and electrophoresis (Pallares et al., 2019). The antimicrobial properties of silver nanoparticles (AgNPs) have resulted in their applications in various fields of medicine, industries, cosmetics, health, animal husbandry, packaging, accessories, and military (Gandhi et al., 2021; Jamila et al., 2021; Kaplan et al., 2022). This increased demand of nanotechnology, motivated the researchers throughout the globe to synthesize novel plants mediated metal nanoparticles instead of using hazardous chemical processes.

Many industrial untreated effluents containing hazardous organic

Peer review under responsibility of King Saud University.
* Corresponding authors.
E-mail addresses: naeem@kust.edu.pk (N. Khan), fakhrakhan82@gmail.com (F. Kalsoom), nargisjamila@sbbwu.edu.pk (N. Jamila), shaukat@kust.edu.pk (S. Shujah), azharulhaq@kust.edu.pk (A. Ul-Haq Ali Shah), umarnishan85@gmail.com (U. Nishan), mishtiaqjan@kust.edu.pk (M. Ishtiaq Jan), imhwang@wikim.re.kr (I. Min Hwang), mohamadsolyman@gmail.com (M.S. Elshikh), rullah@ksu.edu.sa (R. Ullah).

https://doi.org/10.1016/j.jksus.2023.102999
Received 31 August 2023; Received in revised form 25 September 2023; Accepted 8 November 2023
Available online 10 November 2023

dyes which must also be degraded. It has been reported that dyes are continuously polluting freshwater resources and, thus, posing serious threat to life (Danner et al., 2019). Degradation of dyes via nanoparticles has been reported in literature as easy safe, nontoxic and cost effective method (Kapoor et al., 2021; Ravichandran et al., 2022). Recently researchers have reported serious threats about antibiotics contamination which needs to be monitored and controlled (Liu et al. 2021). Colourimetric sensing technique in which nanoparticles are used as a probe is used to detect antibiotics, is believed low-cost, high sensitive, and easy to use (Abedalwafa et al., 2019).

Antibiotics treat antibacterial infections such as urinary tract, ear, lungs, throat and chest infections, tonsils, bronchitis, and many other types of bacterial infections. However, improper use of antibiotics leads to contaminate water and environment. The intake of these antibiotics by humans through different routes causes serious health effects. Therefore, for their removal, cost-effective and affordable methods needs to be developed.

Micromeria biflora is a flowering plant belonging to Labiatae family which is also known as lemon-scented thyme, Jangli Ajwan, Dhawa Jari, and Shamakay (Duru et al., 2004; Sajad et al., 2020). In Pakistan, this plant is found in Swat, Shogran, Kaghan, Dir, and Hazar Nao Hills of Malakand (Ummara et al., 2013; Zeb et al., 2015; Zeb et al., 2016). It has a specific scent due to the presence of terpenoids and a great amount of essential oil (Ding et al., 1994; Mallavarapu et al., 1997; Slavkovska et al., 2005) and also is a source of tannins, flavonoids, and coumarins (Uddin et al., 2016). The plant is traditionally used to treat nosebleed, decay of teeth, wounds healing, headache, different skin infections, treating common cold and sinusitis conditions (Sajad et al., 2020). Considering the unique medicinal applications and novelty of untapped nanostructural study on the subject *M. biflora* plant, this study was therefore aimed to synthesize gold (MBAuNPs) and silver nanoparticles (MBAgNPs) using aqueous extracts of the *M. biflora* plant under conditions of sunlight, stirring, incubation, and heating. The synthesized NPs were characterized and evaluated for their potential in degradation of dyes, and antibiotics, which includes levofloxacin, amoxicillin, and azithromycin, and detection in biological (blood and urine) and water samples.

2. Methods and materials

2.1. Samples collection

Enough aerial parts of *M. biflora* plant was collected from Swat, during the flowering season (June to August 2021) from Swat valley, KPK province, Pakistan. The plant was taxonomically identified at the Botany Department, Peshawar University, Pakistan. The plant was washed to clean from any dust or other contaminants. The samples were then air dried in shade, powdered, kept in dry and cleaned, plastic bags, properly labelled, and stored in refrigerator until analysis. Approval from ethical committee, Kohat University of Science & Technology was obtained for working with biological samples including blood plasma and urine.

2.2. Aqueous extract preparation

For extraction, an established procedure from literature was followed (Jamila et al., 2020). Briefly, deionized water (500 mL) as extraction solvent was used to soak 25 g aerial parts of *M. biflora* powder. The mixture was stirred well at 500 rpm for 2 h and 40 °C temperature. The extract so obtained was filtered, and used to synthesize MBAuNPs and MBAgNPs.

2.3. Chemicals, reagents, and instrumentation

Gold(III) chloride salt as trihydrate ($HAuCl_4{\cdot}3H_2O$), nitrate salt of silver ($AgNO_3$), sodium borohydride ($NaBH_4$), dyes [methylene blue (MB), Congo red (CR), Rhodamine (RdB), methyl orange (MO), and *ortho*- and *para*-nitrophenol (ONP, PNP)], antibiotic standards [levofloxacin (LFX), amoxicillin (AMX), and azithromycin were all purchased from Merck (Darmstadt, Germany) and Sigma-Aldrich (Steinheim, Germany). Aqueous plant extract and all reagent solutions were prepared with ultrapure deionized water obtained from Milli-Q apparatus (Millipore, MA, USA).

Instruments used in this research study included UV–1800 spectrophotometer (Shimadzu, Japan) for absorption spectra (200 to 800 nm) of the reaction mixture, FT-IR spectrometer (Bruker) for functional groups identification (400–4000 cm^{-1}), field emission-scanning electron microscope (FE-SEM, S-4800, Hitachi, Japan), transmission electron microscope (Phillips CM12, Eindhoven, Netherlands) and atomic force microscopy (AFM) for size and morphology assessment.

2.4. Synthesis and characterization of MBAuNPs and MBAgNPs

The MBAuNPs and MBAgNPs were synthesised using *M. biflora* aqueous extract under different conditions involving ratios (1:5 to 1:15) of corresponding salt solutions ($HAuCl_4{\cdot}4H_2O$ and $AgNO_3$) and aqueous extract, sunlight, incubation at 25 °C in dark, stirring, heating, pH (1–12) and time intervals (0 to 180 min). Synthesis of corresponding NPs were preliminary checked for any visible colour change from yellow (extract) to brown (AgNPs) and maroon/deep purple (AuNPs) (Fig. 1), which were then confirmed by UV–Vis analysis. The synthesized NPs from the solutions were collected via centrifugation and washing with water. The product so obtained was kept in sealed vials until required for analysis. The synthesized NPs were characterized by FE-SEM, FT-IR, AFM, and TEM techniques for functional group identification (involved in NPs synthesis), and size and morphology analysis.

2.5. Dyes degradation by MBAuNPs and MBAgNPs

Dyes degradation was evaluated using synthesized NPs (where they act as catalysts) following reported literature (Jamila et al., 2020). Briefly, 0.1 mM, 2.5 mL each of dyes and nitrophenols were mixed with 0.1 mM, 0.5 mL of $NaBH_4$. In another experiment, 3 mg of NPs were mixed with 2.5 mL of solutions of dyes and nitrophenols and 0.5 mL $NaBH_4$. The Ultraviolet–Visible spectra (200–800 nm) were recorded at a time intervals of 0 to180 min. The catalytic efficiency of NPs and degradation of dyes and nitrophenols was noted by discoloration and decrease in SPR absorbance. This decrease was calculated as reduction/decolorization via equation (1) given below.

$$\%decolourization/reduction = (1 - A_t/A_0) \times 100 \quad (1)$$

Where; A_t means absorbance of dye at "t" time and A_0 means absorbance of dye at 0 min.

2.6. Colourimetric antibiotics detection by MBAuNPs and MBAgNPs

In antibiotic detection in real samples, a slightly modified method (Makropoulou et al., 2020) was used. Depending on the solubility, the working solutions were set by taking the selected antibiotics and dissolving either in water or ethanol. The UV spectra of antibiotics working solutions (2.5 mL), a mixture of antibiotics (2.5 mL) and NPs (3 mg), and a mixture of antibiotics working solutions, NPs (3 mg) and real samples (blood plasma, urine, tape water, 1.5 mL) were recorded at 0 to180 min. To evaluate the percent removal of the applied antibiotics, the following equation was used.

$$R\% = (C_0 - C)/C_0{*}100 \quad (2)$$

Where C and C_0 are the final and initial concentrations of the applied antibiotics, respectively.

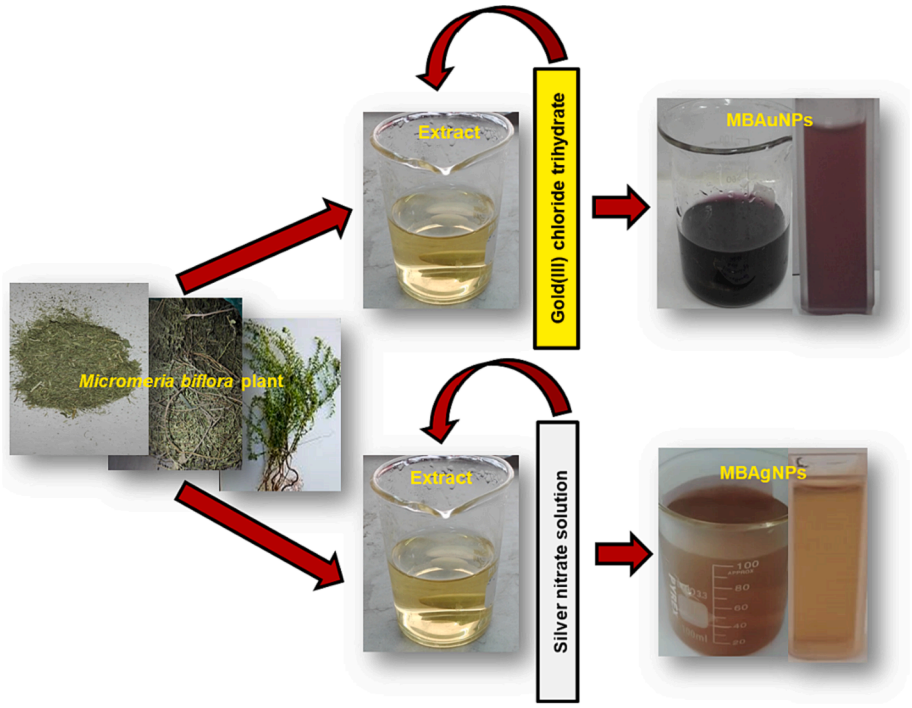

Fig. 1. Colourimetric visible changes in the synthesis of MBAuNPs and MBAgNPs at sunlight.

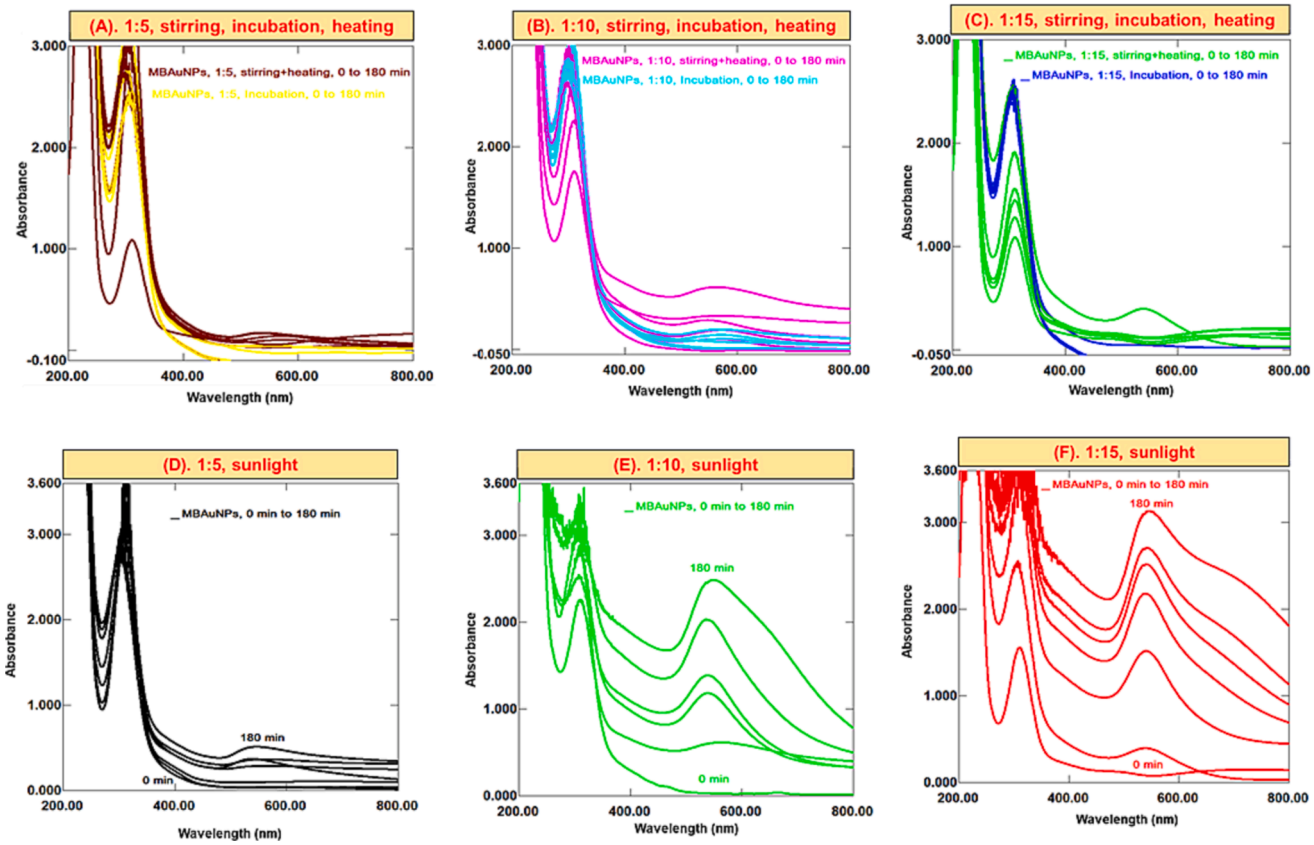

Fig. 2. Successive UV–Vis spectra of MBAuNPs using aqueous extract in ratios of (A) 1:5, (B) 1:10 and (C) 1:15 at stirring, heating, incubation, (D) 1:5 sunlight, (E) 1:10 sunlight, and (F) 1:15 sunlight.

3. Results and discussion

3.1. Synthesis and characterization of MBAuNPs and MBAgNPs

M. biflora mediated NPs were synthesized using various ratios of extract and corresponding salt solutions under sunlight, stirring, incubation, and heating techniques. Applying these conditions to mixtures of 1:5, 1:10, and 1:15 ratios, for MBAuNPs, no visible colour change was noticed, and from UV–Vis study there was no surface plasmon resonance band seemed, which indicates that no NPs in the subject mixtures/ratios are produced at stirring, incubation, and heating as depicted from Fig. 2 (A-C). The prominent SPR peak appeared at λ_{max} 300–350 nm shown in Fig. 2 is attributed to aggregation of particles of sizes larger than 100 nm (Dzimitrowicz et al., 2019). Proceeding the synthesis in sunlight, MBAuNPs were produced at a slow rate in ratio of 1:5 with the more intense SPR at λ_{max} 300–350 nm than at λ_{max} 541 nm (Fig. 2D). However, in 1:10 and 1:15 ratios, significant MBAuNPs were produced as indicated by visible colourimetric change in color from light yellow to purple, and appearance of SPR band at 541 nm (Fig. 2E & F). An intense absorption peak at λ_{max} 541 nm was observed for MBAuNPs produced at the ratio of 1:15, indicating the presence of reasonable AuNPs.

In MBAgNPs synthesis, the colorimetric change from yellow to brown at the ratios of 1:5, 1:6, and 1:7 keeping in sunlight play a crucial role in preparation of MBAgNPs, which exhibited SPR at λ_{max} 431 nm (Fig. 3A & B). A 1:6 ratio demonstrated an intense and sharp SPR band, which indicate the production of significant and well dispersed AgNPs. In a ratio of 1:7, a bathochromic/red shift from 431 to 579 nm and broadened SPR band was observed. Furthermore, due to boosted interactions between MB aqueous extract with excessive amounts of phytocompounds and silver ions, this aggregation ultimately resulted in the decrease of stable MBAgNPs (Lee et al., 2019; Rani et al., 2020). Proceeding with increased salt concentration to 1:10, 1:12, and 1:15, at sunlight, the AgNPs showed weak SPR band (Fig. 3C) and produced at a slow rate, which indicate its formation in small amount. Following the AgNPs synthesis with all the subject ratios at stirring, incubation, and heating, no SPR excitations at 420–450 nm were seen, which corresponded to no AgNPs production (Fig. 3D).

M. biflora is a rich source of chemical constituents/secondary metabolites such as phenolics, tannins, flavonoids, and coumarins (Chandra et al. 2013). The hypothesised mechanism for the NPs synthesis by the interaction of these secondary metabolites with metal ions include interaction of OH/COOH/NH groups, enol synthesis by liberating reactive hydrogen, and then oxidation of hydroxyl to carbonyl group through adsorption on the metal surface (Kumar et al., 2017). The metal ions $M^{+/++}$ thus are reduced to M^0, and eventually NPs creation. According to Lee et al. (2019), nanomaterials synthesized via these

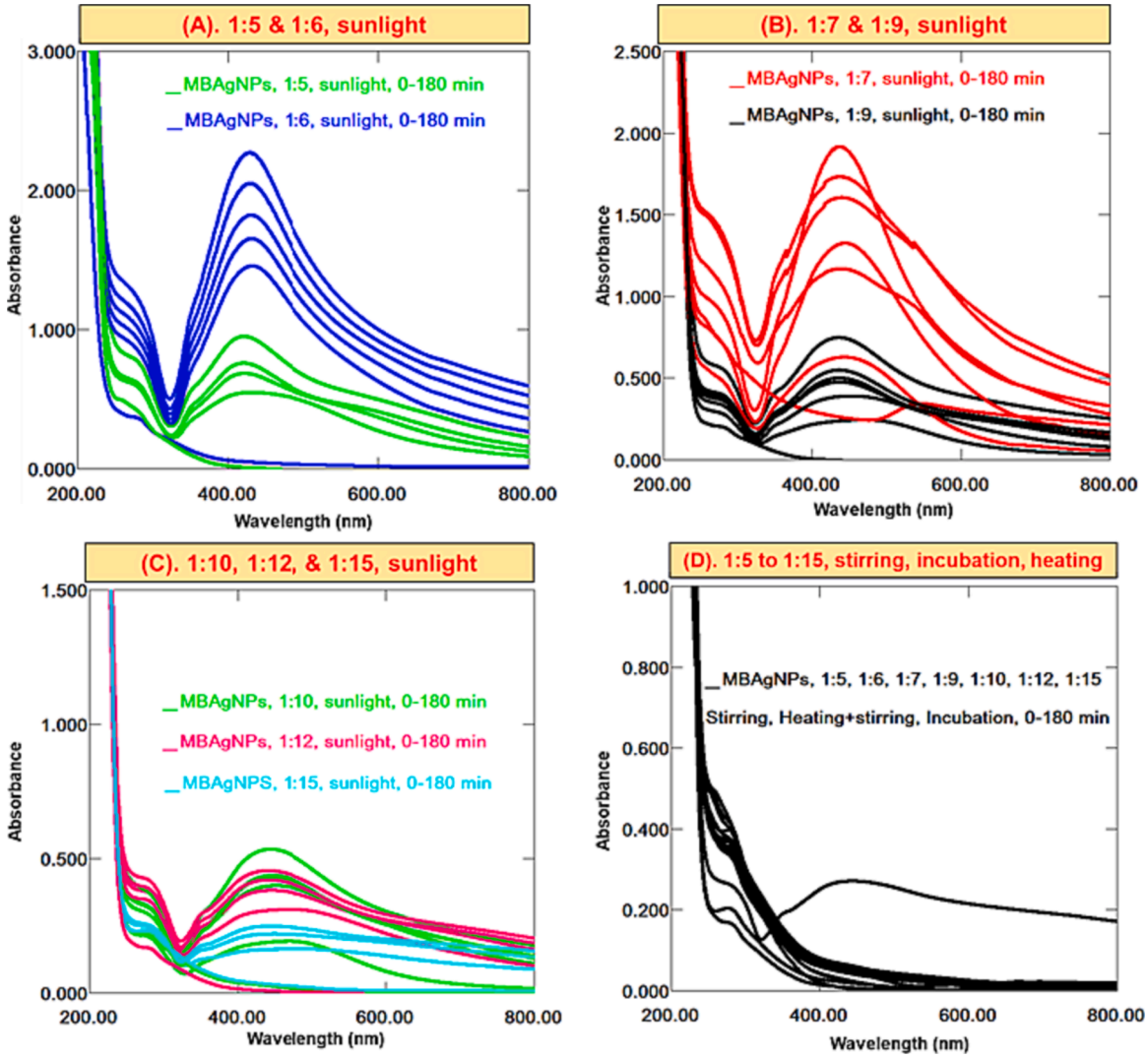

Fig. 3. Successive UV–Vis spectra of MBAuNPs using aqueous extract in ratios of (A) 1:5 & 1:6 sunlight (B) 1:7 & 1:9 sunlight, (C) 1:10, 1:12 & 1:15 sunlight, (D) 1:5 to 1:15 at stirring, heating, and incubation.

bioactive components, which have hydroxyl groups as reducing agents follow the mechanism as shown below.

$$Au^{+} + R - OH \rightarrow Au^{0} + R = O + H^{+}$$

$$R - OH + Ag^{+} \rightarrow Ag^{0} + H^{+} + R = O$$

Depending upon the extent and position of both hydroxyl and carbonyl functional groups in the plant constituents, the NPs synthesis and their biological activities are greatly affected. Regarding the synthesis of MBAuNPs, the interaction of Au^{+} with phenolics of *M. biflora* extract, the colorimetric colour change from yellow to purple indicate the reduction of Au^{+} to Au, and hence, MBAuNPs production. MBAuNPs synthesized under sunlight were significantly produced in 1:10 and 1:15 ratios, exhibiting surface plasmon resonance (SPR) band at 541 nm, as indicated by previous literature (Dzimitrowicz et al., 2019; Rani et al., 2020). In 1:15 ratio, MBAuNPs were produced in the highest extent. Hence, it is the optimal ratio displaying a sharp absorption peak at λ_{max} 541 nm. This indicates that the salt solution ($HAuCl_4$) is rapidly reduced by the chemical constituents of *M. biflora* to produce homogeneous nuclei, which results in tiny AuNPs rather than aggregates.

Concerning MBAgNPs in 1:6 ratio under sunlight, which display a sharp peak at λ_{max} 431 nm, shows that this ratio is the optimal condition for the synthesis of MBAgNPs. However, proceeding to higher ratios, a bathochromic/red shift from 431 to 579 nm and a broadened SPR band was observed, which indicates salt induced MBAgNPs aggregation. Also due to greater interactions between *M. biflora* aqueous extract with excessive amounts of reducing phytoconstituents and accessible silver ions, this aggregation finally resulted in the reduction of stable MBAgNPs which is consistent to the published literature (Lee et al., 2019). Similarly, Rani et al. (2020) has reported about Ostwald slow ripening process to enhance the production of AgNPs and result in size enlargement. Owing to several properties, many of the NPs have been used for the pollutants detection; dyes, antibiotics (Zhang et al., 2020; Aguilar-Pérez et al., 2021).

The functional groups of the phytochemicals (tannins, flavonoids, coumarins) present in *M. biflora*, which involve in the synthesis of *M. biflora* nanoparticles (MBNPs) were evaluated using FT-IR technique. The FT-IR spectra of plant extract (MBAE) are labelled by comparing with literature (Fig. 4A & B). The broad and intense absorption bands at 3500–3200 cm^{-1} is the stretching vibration assigned to hydroxyl (–OH), and or amine (–NH) groups however the absorption frequencies at 1700–1540 cm^{-1} and 1030–13010 cm^{-1} are attributed to –C = O and –C–O stretching vibrations. It has been observed that the subject absorption bands in the spectra of MBAuNPs and MBAgNPs either reduced or disappeared, thus concluding the contribution of the different functionalities in MBNPs synthesis (Jamila et al., 2020).

The morphology and size of the subject MBNPs were analyzed using TEM, SEM and AFM techniques. These techniques showed that the size

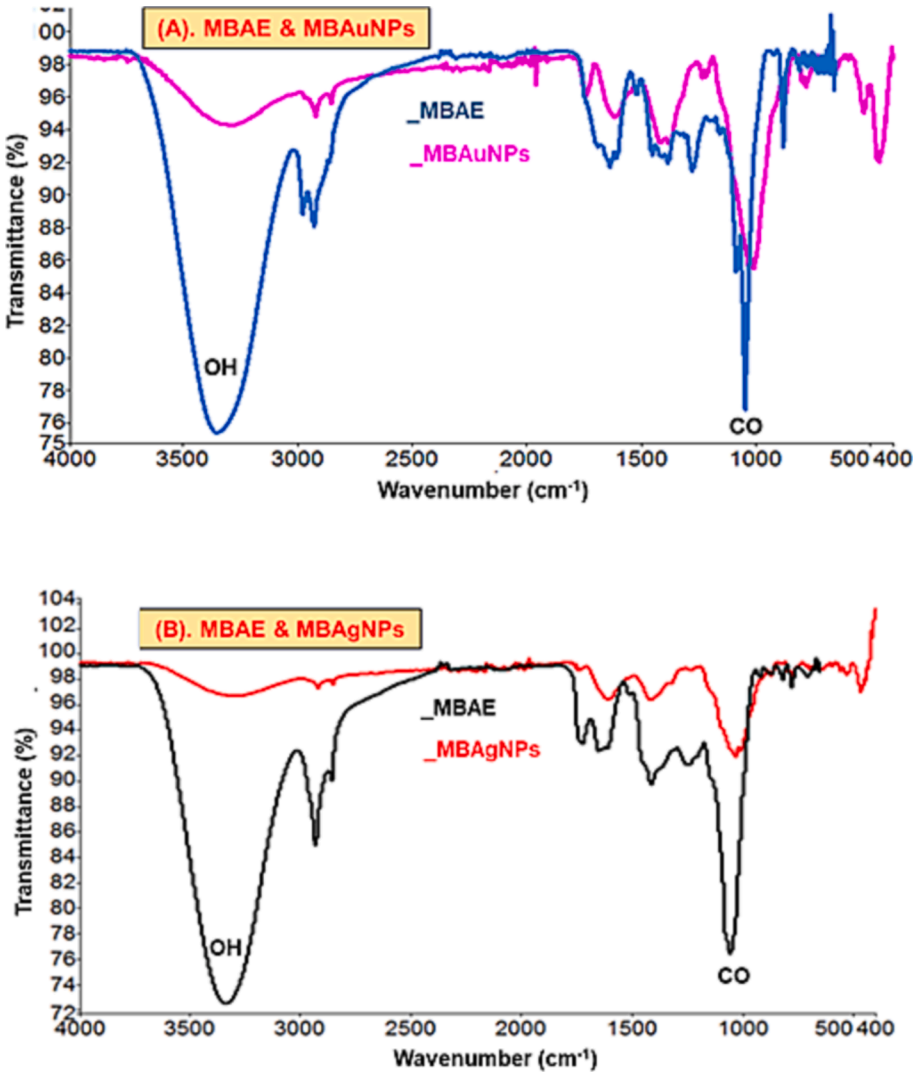

Fig. 4. FT-IR spectra of (A) MBAE and MBAuNPs, and (B) MBAE and MBAgNPs.

of MBAuNPs is 26.73 nm, and the surface shape represented nanorods as well as spherical shapes (Fig. 5A-C). Regarding MBAgNPs, the size by the subject techniques was found to be 53.81 nm with spherical shape (Fig. 5D-F).

3.2. Catalytic activity of MBAuNPs and MBAgNPs in dyes degradation

In the current study, CR, MB, MO, RdB, ONP, and PNP were reduced using $NaBH_4$ and MBNPs. The combined UV–Vis spectra of dyes reduced with $NaBH_4$, and MBAuNPs and AgNPs (Fig. 6) explained that dyes without MBNPs have a little variability in absorbance with no noticeable change in colour was observed, which indicates a slow rate of degradation of dyes reduction. However, MBAuNPs added dyes exhibited spectra where certain absorption peaks disappeared within 5 min after the addition of MBNPs. The results of the subject dyes (Fig. 6) showed that MB (cationic dye), which displays λ_{max} at 653 nm, 591 nm, and 290 and inefficiently reduced by $NaBH_4$, the absorbance at 653 and 290 nm weakened with a concurrent increase at 255 nm after the MBNPs addition (Fig. 6A). Similarly, the absorption maxima of CR (λ_{max} at 487 and 349 nm), RdB (550 nm), and MO (λ_{max} at 462 nm) decrease and shift to blue shift with the addition of MBNPs (Fig. 6B-D). The *ortho*-nitrophenol and *para*-nitrophenols (Fig. 6E & F) also have shown high degradation rate for ONP followed by PNP. MBAuNPs reduced CR to 80–85 %, MB 70–75 %, RdB 15–20 %, MO 65–80 %, ONP 80–85 %, and PNP 80–85 %. Regarding the % degradation of dyes by MBAgNPs (Fig. 7), the dyes were reduced as follows: CR (75–80 %), RdB (15–20 %), MB (60–70 %), MO (80–85 %), PNP (80–85 %), and ONP (83–85 %).

Dyes are the organic synthetic pollutants, which release into the running water by various industries (Sadia et al., 2023). These dyes are polluting water and absorbed by soil thus affecting the environment, human health, and agriculture. Therefore, to control and cope this issue, recently, NPs of well enough catalytic efficiency have played key role as effective catalysts in the discolouration and elimination by decreasing the activation energy (Jamila, 2020; Khan et al., 2021; Yıldırım et al., 2022). The synthetic reducing agent ($NaBH_4$), which is usually used to reduce dyes due to the large redox potential differences in the dye and BH_4^- ions, inefficiently reduce dyes. Therefore, due to the adsorption of dyes on NPs, the electron transfer from $NaBH_4$ to dyes becomes easy and dye molecules decolorize. This is attributed to the high catalytic locations, lower the activation energy, and high volume to surface ratio of NPs. This diagram depicts MB-AuNPs' catalytic characteristics (Wang et al., 2021).

In this analysis, the λ_{max} of dyes are decreased, which indicates the degradation of dyes. For example, for CR (Figs. 6 and 7A), showing λ_{max} at 487 and 349 nm, the absorbance at the subject λ_{max} decreased and the solution become faint. In MB dye (Figs. 6 and 7B) having λ_{max} 653 and 290 nm, the absorbance decreased with an appearance of another absorption peak at 255 nm. This simultaneous decrease/increase in the λ_{max} indicates dyes degradation.

3.3. Antibiotics detection by MBAuNPs and MBAgNPs

The most used antibiotics selected for this study including LFX, AMX, and AZM in water, blood plasma and urine samples were detected using both type of NPs as a probe. From the results (Figs. 8 and 9), it was found that upon the addition of MBNPs to the antibiotics solution, the concentration (absorbance) of the mixtures decreases. AMX solution displays absorption peaks at λ_{max} 228 nm and 277 nm. Upon the addition of MBNPs, antibiotics are adsorbed on their surface and the λ_{max} of antibiotics decreases. Regarding the other antibiotics, it can also be seen that the same changes/decrease in λ_{max} occurs. In this study, it was found that compared to AZM, AMX and LFX capture by MBNPs was significant, and the removal % was in the range of 75–85 %. Proceeding the experiments with aqueous medium (tap water), blood plasma and urine samples, the recorded spectra obtained were irregular, and indicated that the λ_{max} of antibiotics decreases, which in turn shows decrease in concentrations of antibiotics.

Antibiotics are also considered as the environmental pollutants from different pharmaceutical industries, various sewage treatment plants, hospitals, and others that can have an impact on microbial ecosystems. Therefore, it is crucial to assess and develop methods for their removal from the environment. Due to the outstanding affinity and optical absorbance of NPs with biomaterials, these have served as an effective technique to identify a variety of chemicals such as -agonists, dopamine, antibiotics, proteins, and DNA. Also, in current study, MBAuNPs and MBAgNPs were used for antibiotics detection in this study. The antibiotics (levofloxacin, amoxicillin, and azithromycin) have a high affinity for *M. biflora* phytoconstituents due to hydrogen-bonding interactions as previously reported by Lai et al. (2017). This results in cross-linking of AuNPs and AgNPs, leading to clear changes in absorbance features and colour. As given in Figs. 8 and 9, a colorimetric assay based on MBNPs as a probe is designed to detect antibiotics including LFX, AMX, and AZM in real samples including water, blood plasma and urine. From the results a decrease in the λ_{max} of antibiotics was found, which is attributed to the interaction via hydrogen bonding of the carboxyl and hydroxyl (COOH and OH) functional groups with antibiotics.

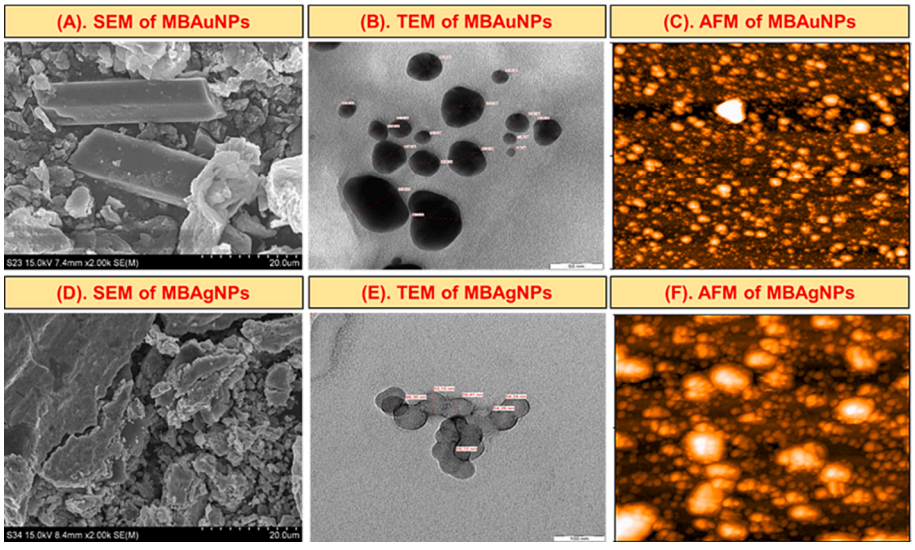

Fig. 5. Size and morphology by (A, D) SEM (B, E), TEM (C, F), AFM images of the synthesized MBAuNPs and MBAgNPs.

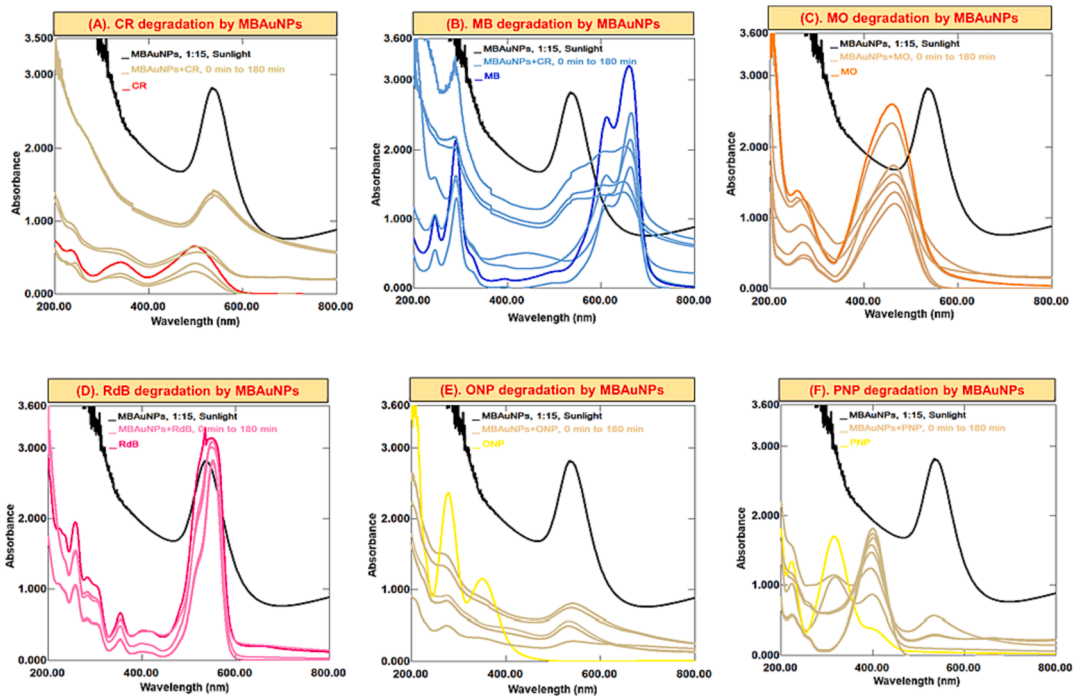

Fig. 6. Successive UV–Vis absorption spectra for the catalytic potential of MBAuNPs in (A) CR, (B) MB, (C) MO, (D) RdB, (E) ONP, (F) PNP in dyes/nitrophenols degradation/reduction process.

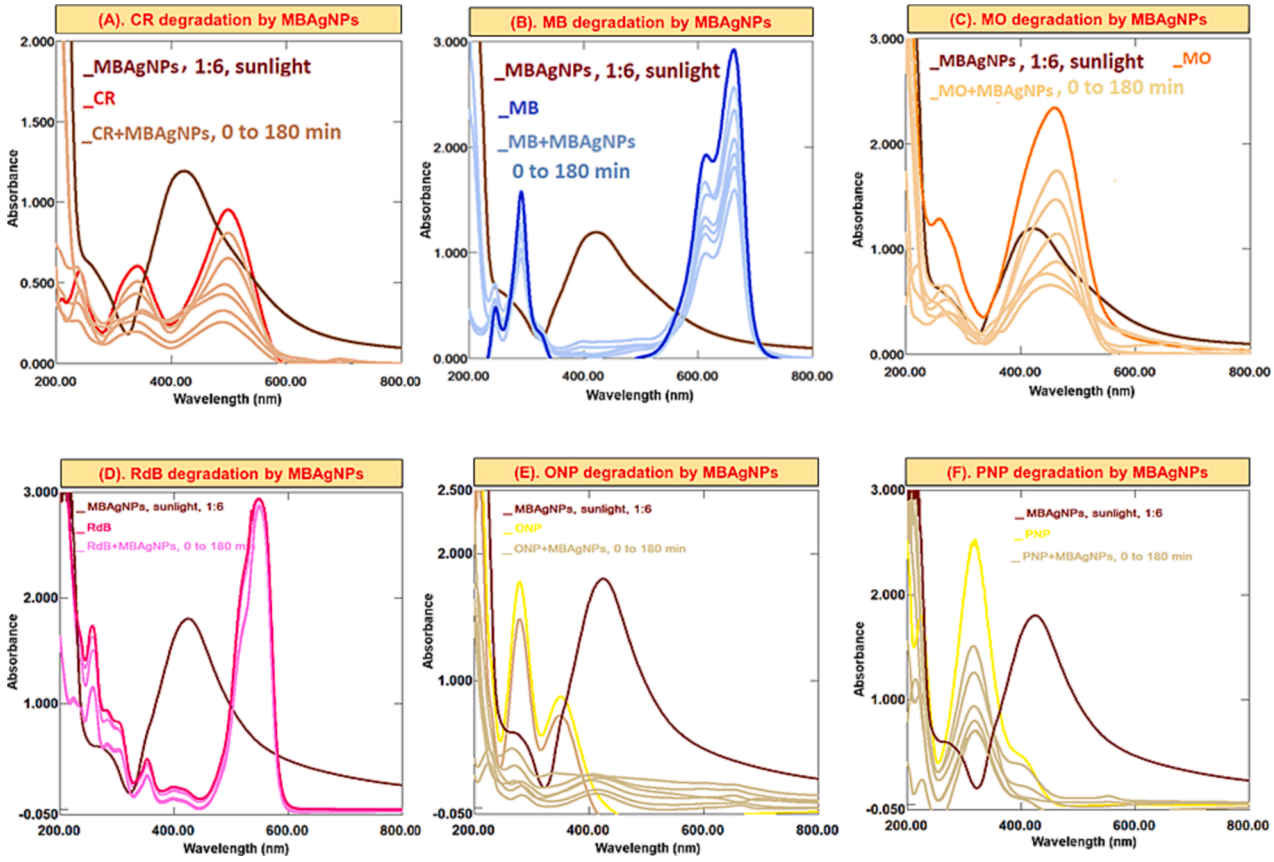

Fig. 7. Successive UV–Vis absorption spectra for the catalytic potential of MBAgNPs in (A) CR, (B) MB, (C) MO, (D) RdB, (E) ONP, (F) PNP in dyes/nitrophenols degradation/reduction process.

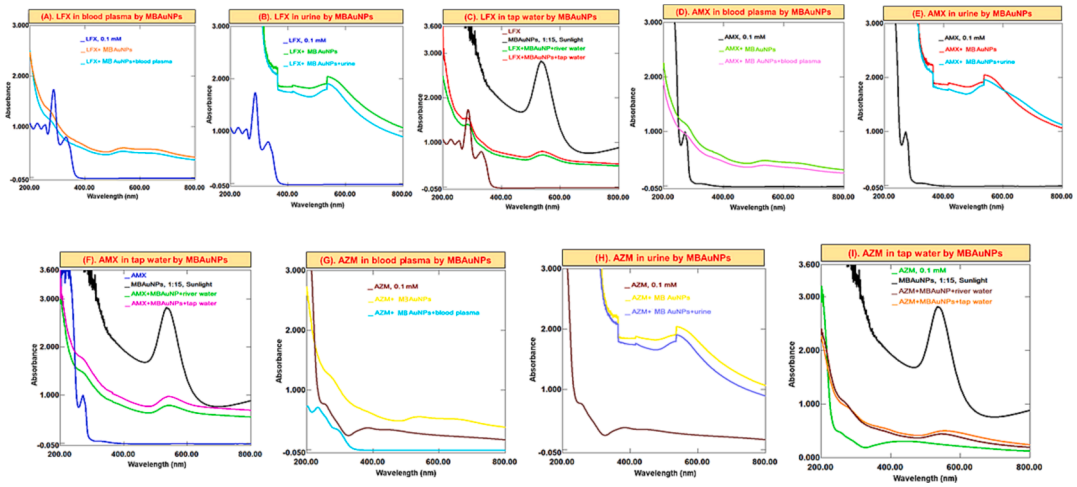

Fig. 8. Successive UV–Vis absorption spectra of MBAuNPs interaction with (A-C) LFX (D-F) AMX, and (G-I) AZM in in blood, urine and water.

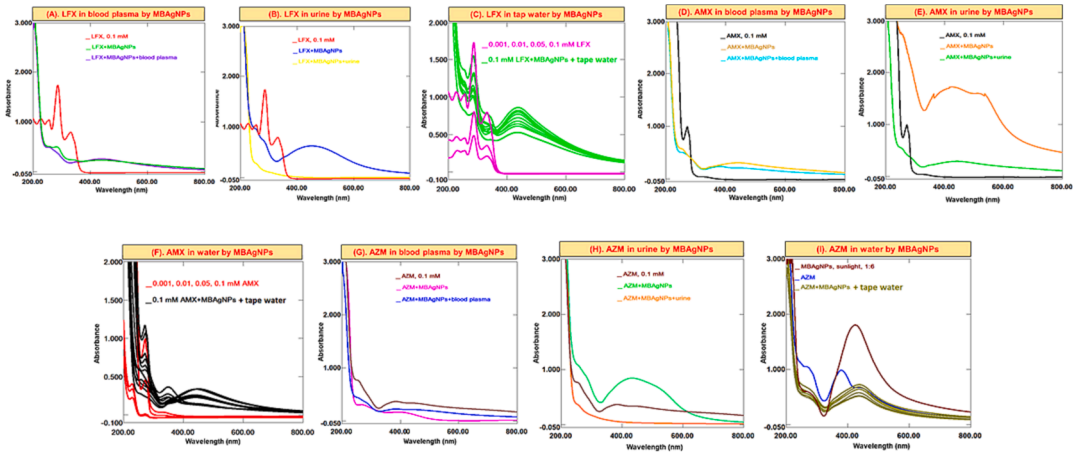

Fig. 9. Successive UV–Vis absorption spectra of MBAgNPs interaction with (A-C) LFX (D-F) AMX, and (G-I) AZM in in blood, urine and water.

From experiments, it was found that the decrease in the absorbance (concentration) of the LFX, AMX, and AZM solutions and MBNPs occurs. This shows that the concentration decrease because of the antibiotics adsorption on the MBNPs then ultimately lead to removal of the studied antibiotics from real samples as also suggested by published studies (Lai et al., 2017; Abedalwafa et al., 2019a; Makropoulou et al., 2020).

4. Conclusions

Conclusively, this study reported the green synthesis of AuNPs and AgNPs using *M. biflora* aqueous extract. The synthesized MBNPs were evaluated for their practical application in dyes/nitrophenols degradation, and antibiotics removal. The subject synthesized MBNPs degraded dyes to 60–87 %. Furthermore, the MBNPs also displayed efficient activity in removal of antibiotics from aqueous and biological media to an extent of 75–85 %. The subject study depicts that MBNPs could be efficient adsorbent dyes/nitrophenols degradation, and antibiotics removal both from aqueous as well as biological samples. Hence, it could provide a better way to control environmental/water pollution, and health problems for the developing countries specifically Pakistan.

Declaration of Competing Interest

The authors declare that they have no known competing financial interests or personal relationships that could have appeared to influence the work reported in this paper.

Acknowledgement

Authors wish to thank researchers supporting project pumber (RSP2023R110) at King Saud University Riyadh, Saudi Arabia for financial support.

References

Abedalwafa, M.A., Li, Y., Ni, C., Wang, L., 2019. Colorimetric sensor arrays for the detection and identification of antibiotics. Anal. Methods 11, 2836–2854. https://doi.org/10.1039/C9AY00371A.

Aguilar-Pérez, K., Avilés-Castrillo, J., Ruiz-Pulido, G., Medina, D.I., Parra-Saldivar, R., Iqbal, H.M., 2021. Nanoadsorbents in focus for the remediation of environmentally-related contaminants with rising toxicity concerns. Sci. Total Environ. 779, 146465 https://doi.org/10.1016/j.scitotenv.2021.146465.

Ansari, A.A., Parchur, A.K., Chen, G., 2022. Surface modified lanthanide upconversion nanoparticles for drug delivery, cellular uptake mechanism, and current challenges in NIR-driven therapies. Coord. Chem. Rev. 457, 214423 https://doi.org/10.1016/j.ccr.2022.214423.

Báez, D.F. Gallardo-Toledo, E., Oyarzún, M.P. Araya, E., Kogan, M.J. (2021). The influence of size and chemical composition of silver and gold nanoparticles on *in vivo* toxicity with potential applications to central nervous system diseases. Int. J. Nanomed. 16, 2187. 10.2147%2FIJN.S260375.

Chandra, M., Prakash, O., Bachheti, R.K., Kumar, M., Pant, A.K., 2013. Essential oil composition and pharmacological activities of Micromeria biflora (Buch.- Ham. Ex D. Don) Benth. collected from Uttarakhand region of India. J. Med. Plant Res. 7, 2538–2544. http://www.academicjournals.org/JMPR.

Danner, M.-C., Robertson, A., Behrends, V., Reiss, J., 2019. Antibiotic pollution in surface fresh waters: occurrence and effects. Sci. Total Environ. 664, 793–804. https://doi.org/10.1016/j.scitotenv.2019.01.406.

Ding, J., Xuejian, Y., Yu, W., Ding, Z., Chen, Z., Hayashi, N., Komae, H., 1994. Aromatic components of the essential oils of four Chinese medicinal plants (Asarum petelotii, Elsholtzia souliei, Eupatorium adenophorum, Micromeria biflora) in Yunnan. Z. Naturforsch. *C*. 49, 703–706. https://doi.org/10.1515/znc-1994-11-1202.

Duru, M.E., Öztürk, M., Uğur, A., Ceylan, Ö., 2004. The constituents of essential oil and *in vitro* antimicrobial activity of *Micromeria cilicica* from Turkey. J. Ethnopharmacol. 94, 43–48. https://doi.org/10.1016/j.jep.2004.03.053.

Dzimitrowicz, A., Berent, S., Motyka, A., Jamroz, P., Kurcbach, K., Sledz, W., Pohl, P., 2019. Comparison of the characteristics of gold nanoparticles synthesized using aqueous plant extracts and natural plant essential oils of *Eucalyptus globulus* and *Rosmarinus officinalis*. Arab. J. Chem. 12, 4795–4805. https://doi.org/10.1016/j.arabjc.2016.09.007.

Gandhi, A.D., Miraclin, P.A., Abilash, D., Sathiyaraj, S., Velmurugan, R., Zhang, Y., Soontarapa, K., Sen, P., Sridharan, T., 2021. Nanosilver reinforced *Parmelia sulcata* extract efficiently induces apoptosis and inhibits proliferative signalling in MCF-7 cells. Environ. Res. 199, 111375 https://doi.org/10.1016/j.envres.2021.111375.

Jamila, N., Khan, N., Bibi, A., Haider, A., Khan, S.N., Atlas, A., Nishan, U., Minhaz, A., Javed, F., Bibi, A., 2020. *Piper longum* catkin extract mediated synthesis of Ag, Cu, and Ni nanoparticles and their applications as biological and environmental remediation agents. Arab. J. Chem. 13, 6425–6436. https://doi.org/10.1016/j.arabjc.2020.06.001.

Jamila, N., Khan, N., Hwang, I.M., Saba, M., Khan, F., Amin, F., Khan, S.N., Atlas, A., Javed, F., Minhaz, A., 2020. Characterization of natural gums via elemental and chemometric analyses, synthesis of silver nanoparticles, and biological and catalytic applications. Int. J. Biol. Macromol. 147, 853–866. https://doi.org/10.1016/j.ijbiomac.2019.09.245.

Jamila, N., Khan, N., Bibi, N., Waqas, M., Khan, S.N., Atlas, A., Amin, F., Khan, F., Saba, M., 2021. Hg (II) sensing, catalytic, antioxidant, antimicrobial, and anticancer potential of Garcinia mangostana and α-mangostin mediated silver nanoparticles. Chemosphere 272, 129794. https://doi.org/10.1016/j.chemosphere.2021.129794.

Kaplan, Ö., Tosun, N.G., İmamoğlu, R., Türkekul, İ., Gökçe, İ., Özgür, A., 2022. Biosynthesis and characterization of silver nanoparticles from *Tricholoma ustale* and *Agaricus arvensis* extracts and investigation of their antimicrobial, cytotoxic, and apoptotic potentials. J. Drug Deliv. Sci. Technol. 69, 103178 https://doi.org/10.1016/j.jddst.2022.103178.

Kapoor, R.T., Salvadori, M.R., Rafatullah, M., Siddiqui, M.R., Khan, M.A., Alshareef, S.A., 2021. Exploration of microbial factories for synthesis of nanoparticles–a sustainable approach for bioremediation of environmental contaminants. Front. Microbiol. 12, 1404. https://doi.org/10.3389/fmicb.2021.658294.

Khan, S.A., Bakhsh, E.M., Asiri, A.M., Khan, S.B., 2021. Synthesis of zero-valent Au nanoparticles on chitosan coated NiAl layered double hydroxide microspheres for the discoloration of dyes in aqueous medium. Spectrochim. Acta A 250, 119370. https://doi.org/10.1016/j.saa.2020.119370.

Kumar, B., Smita, K., Cumbal, L., Debut, A., 2017. Green synthesis of silver nanoparticles using Andean blackberry fruit extract. Saudi J. Biol. Sci. 24, 45–50. https://doi.org/10.1016/j.sjbs.2015.09.006.

Lai, C., Liu, X., Qin, L., Zhang, C., Zeng, G., Huang, D., Cheng, M., Xu, P., Yi, H., Huang, D., 2017. Chitosan-wrapped gold nanoparticles for hydrogen-bonding recognition and colorimetric determination of the antibiotic kanamycin. Microchim. Acta 184, 2097–2105. https://doi.org/10.1007/s00604-017-2218-z.

Lee, K.X., Shameli, K., Mohamad, S.E., Yew, Y.P., Mohamed Isa, E.D., Yap, H.-Y., Lim, W. L., Teow, S.-Y., 2019. Bio-mediated synthesis and characterisation of silver nanocarrier, and its potent anticancer action. Nanomaterials 9, 1423. https://doi.org/10.3390/nano9101423.

Liu, C., Tan, L., Zhang, L., Tian, W., Ma, L., 2021. A review of the distribution of antibiotics in water in different regions of China and current antibiotic degradation pathways. Front. Environ. Sci. 9, 692298 https://doi.org/10.3389/fenvs.2021.692298.

Makropoulou, T., Kortidis, I., Davididou, K., Motaung, D.E., Chatzisymeon, E., 2020. Photocatalytic facile ZnO nanostructures for the elimination of the antibiotic sulfamethoxazole in water. J. Process. Eng. 36, 101299 https://doi.org/10.1016/j.jwpe.2020.101299.

Mallavarapu, G.R., Ramesh, S., Subrahmanyam, K., 1997. Composition of the essential oil of *Micromeria biflora*. J. Essent. Oil Res. 9, 23–26. https://doi.org/10.1080/10412905.1997.9700709.

Pallares, R.M., Choo, P., Cole, L.E., Mirkin, C.A., Lee, A., Odom, T.W., 2019. Manipulating immune activation of macrophages by tuning the oligonucleotide composition of gold nanoparticles. Bioconjug. Chem. 30, 2032–2037. https://doi.org/10.1021/acs.bioconjchem.9b00316.

Pirtarighat, S., Ghannadnia, M., Baghshahi, S., 2019. Green synthesis of silver nanoparticles using the plant extract of *Salvia spinosa* grown *in vitro* and their antibacterial activity assessment. J. Nanostruct. Chem. 9, 1–9. https://doi.org/10.1007/s40097-018-0291-4.

Rani, P., Kumar, V., Singh, P.P., Matharu, A.S., Zhang, W., Kim, K.-H., Singh, J., Rawat, M., 2020. Highly stable AgNPs prepared via a novel green approach for catalytic and photocatalytic removal of biological and non-biological pollutants. Environ. Int. 143, 105924 https://doi.org/10.1016/j.envint.2020.105924.

Ravichandran, K., Vasanthi, D., Kavitha, P., Shalini, R., Suvathi, S., Praseetha, P., 2022. Cost-effective and eco-friendly dye degradation by enzyme-powered ZnO nanomaterial: effect of process temperature. Bull. Mater. Sci. 45, 1–5. https://doi.org/10.1007/s12034-021-02619-8.

Sadia, M., Ahmad, I., Ul-Saleheen, Z., Zubair, M., Zahoor, M., Ullah, R., Bari, A., Zekker, I., 2023. Synthesis and characterization of MIPs for selective removal of textile dye acid black-234 from wastewater sample. Molecules 28 (4), 1555. https://doi.org/10.3390/molecules28041555.

Sajad, M.A., Khan, M.S., Bahadur, S., Naeem, A., Ali, H., Batool, F., Shuaib, M., Khan, M. A.S., Batool, S., 2020. Evaluation of chromium phytoremediation potential of some plant species of Dir Lower, Khyber Pakhtunkhwa, Pakistan. Acta Ecol. Sin. 40, 158–165. https://doi.org/10.1016/j.chnaes.2019.12.002.

Salem, S.S., Fouda, A., 2021. Green synthesis of metallic nanoparticles and their prospective biotechnological applications: an overview. Biol. Trace Elem. Res. 199, 344–370. https://doi.org/10.1007/s12011-020-02138-3.

Slavkovska, V., Couladis, M., Bojovic, S., Tzakou, O., Pavlovic, M., Lakusic, B., Jancic, R., 2005. Essential oil and its systematic significance in species of *Micromeria Bentham* from Serbia & Montenegro. Plant Systemat. Evol. 255, 1–15. https://doi.org/10.1007/s00606-005-0303-y.

Uddin, G., Rauf, A., Siddiqui, B.S., Khan, H., Barkatullah, U.R., 2016. Antinociceptive, antioxidant and phytochemical studies of Pakistani medicinal plants. Pak. J. Pharm. Sci. 29, 929–933.

Ummara, U., Bokhari, T.Z., Altaf, A., Younis, U., Dasti, A.A., 2013. Pharmacological study of Shogran valley flora, Pakistan. Int. J. Sci. Eng. Res. 4, 1–9.

Wang, G., Zhao, K., Gao, C., Wang, J., Mei, Y., Zheng, X., Zhu, P., 2021. Green synthesis of copper nanoparticles using green coffee bean and their applications for efficient reduction of organic dyes. J. Environ. Chem. Eng. 9, 105331 https://doi.org/10.1016/j.jece.2021.105331.

Yıldırım, R., Karataş, Y., Demirci, U.B., Gülcan, M., 2022. Fabrication and characterization of copper nanoparticles anchored on sulfonated reduced graphene oxide as effective catalyst for the reduction of Thioflavine-T cationic dye in aqueous medium. Mater. Chem. Phys. 275, 125212 https://doi.org/10.1016/j.matchemphys.2021.125212.

Zeb, U., Khan, H., Gul, B., Khan, W.M., 2016. Floristic composition and phytosociological studies of Hazar Nao hills, District Malakand, Khyber Pakhtunkhwa, Pakistan. Pak. J. Weed Sci. Res. 22, 295–315.

Zeb, M.A., Wahab, A., Ullah, N., Jabbar, A., Pandey, S., Muhammad, T., 2015. Antibacterial and antifungal activities of Micromeria biflora (Leaves). Int. J. Med. Biomed. Sci. 1, 28–34. https://doi.org/10.55530/ijmbiosnepal.v1i1.7.

Zhang, S., Li, B., Wang, X., Zhao, G., Hu, B., Lu, Z., Wen, T., Chen, J., Wang, X., 2020. Recent developments of two-dimensional graphene-based composites in visible-light photocatalysis for eliminating persistent organic pollutants from wastewater. Chem. Eng. J. 390, 124642 https://doi.org/10.1016/j.cej.2020.124642.